International Journal for Housing Science and Its Applications
Publish August 4, 2025. Volume 46, Issue 3 Pages 2143-2152

https://doi.org/10.70517/ijhsa463170

Modeling and computational method analysis of carbon nanomaterials enhanced microbial fuel cell for treatment of complex wastewater

Weicheng Wen[1], Chundi Ma[1], Tianfu Shao[1], Jiangyiye Li[2], Yiyang Li[1] and Wenhua Piao[1,*]
[1] College of Geography and Ocean Sciences, Yanbian University, Hunchun, Jilin, 133300, China
[2] Agricultural College, Yanbian University, Yanji, Jilin, 133000, China
Corresponding authors: (e-mail: piaowenhua66@163.com).

Abstract Enhancing the treatment capacity of complex wastewater has a contributing role to the green development of the environment. In this paper, the wastewater treatment capacity of microbial fuel cells is enhanced based on the excellent properties of nanocarbon materials. Nitrogen-doped porous carbon materials and biomass carbon materials are prepared as the material basis for the modified anode of the cell. The microbial fuel cells were constructed and the effluent treatment capabilities of the three types of cells, L-N/PCs-MFC, N/PCs-MFC, and PCs-MFC, were compared by multiple sets of experiments. The electrochemical performance of L-N/PCs-MFC was analyzed based on cyclic voltammetry, polarization and power density tests. The water purification effect of L-N/PCs-MFC was verified by COD, TP, and TN removal tests. The results showed that the CV curves of L-N/PCs anode showed obvious redox peaks at both -0.45 V and 0.5 V voltage, which was higher than the capacitance. The open-circuit voltage was 820.59 mV and the slope was smaller than that of the comparison cell, and the internal resistance was minimized during the operation. The removal rates of COD, TP, and TN were all higher, and the water purification effect was good and could maintain the microbial activity effectively.

Index Terms carbon nanomaterials, microbial fuel cells, L-N/PCs, electrochemical performance, water purification effect

I. Introduction

In the current process of social functioning, economic development, industrial and agricultural production, and ecosystem circulation, water is one of the crucial elements, as well as in human survival, water is also a core element to reduce diseases and improve environmental quality [1]-[4]. However, along with the rapid development of industrialization and the massive use of water resources, water sanitation problems have arisen. UNESCO pointed out in 2017 that 80% of the sewage wastewater is discharged into the ecosystem without treatment or is not recycled, which puts great pressure on the restoration of the ecological environment [5], [6]. In fact, sewage wastewater is also a kind of resource, the discharged sewage wastewater usually contains a large amount of organic matter, but the conventional wastewater treatment farms are unable to make full use of these resources, instead, they need to consume a large amount of energy to run and operate the wastewater treatment equipment, and if they can make full use of the chemical energy in these organic matter, they can not only reduce the consumption of energy, but also obtain energy from the sewage [7]-[9]. In addition, traditional wastewater treatment technologies usually require a large amount of power supply and chemical inputs, which not only has the problem of energy waste and environmental pollution, but also keeps the cost of wastewater treatment high, which is not conducive to the economic and green development, and limits the treatment sustainability [10]-[12].

In this context, the emergence of microbial fuel cell (MFC) brings a new solution for wastewater treatment with many potential advantages. MFC is a novel bioelectrochemical technology, which can degrade organic nutrients in wastewater through the electricity-producing microorganisms in the anode chamber, and at the same time, release electrons and protons, and the electrons are transferred to the cathode of the fuel cell through the external circuit to realize the energy yield [13]. The advantages of its mild working conditions, green environment, capacity, and low sludge volume have also gradually gained attention and have a broad prospect [14], [15]. However, in practical applications, the poor stability of MFC in long-term working scenarios, high requirements on working environment and electrode materials, and low power generation have hindered the further application of MFC [16]-[18].

While nanocarbon materials bring a new turn to the above problems, nanocarbon materials are carbon materials where the dispersed phase scale has at least one dimension less than 100 nm. The dispersed phase can be composed of either carbon atoms or heterogeneous atoms (non-carbon atoms), or even nanopores. Among the

nanocarbon materials, new carbon materials such as carbon nanofibers, carbon nanotubes, graphene, and carbon quantum dots have excellent physical and chemical properties such as ultra-high specific surface area, three-dimensional porous structure, high electrical conductivity, and catalytic properties, which have been widely used in many fields, and also serve as an effective material for the performance enhancement of MFC [19], [20].

In large-scale application scenarios, the effect of MFCs is constrained by the performance of their anode electrodes. In graphene-based MFC performance enhancement, literature [21] evaluated the effectiveness of a homemade 3D graphene electrode as an anode electrode material for MFCs, obtaining the maximum power density under tetravalent potassium ferricyanide configuration conditions. The nitrogen-doped graphene oxide prepared by literature [22] increased the power density of MFC (708.3 mW/m²), which promoted the bioelectrocatalytic activity and enhanced the wastewater treatment. Literature [23] prepared a low-cost, high-performance composite anode material for MFC by utilizing derivatized graphene from oil palm biomass waste and adding lead-containing wastewater.

In the carbon nanotube-based MFC performance enhancement, literature [24] verified that the modification of multi-walled carbon nanotubes effectively enhanced the maximum power density of MFC (560.40 mW/m²), optimizing the biofilm formation, biodegradation, and electron transfer of the MFC anode with its single-bonded carboxylate group. Literature [25] explained that the large-scale porosity and nanostructure of carbon nanotubes through the woven fiber process colonized electroactive bacteria on the surface of MFC electrodes, which resulted in superior electrode performance than ordinary carbon electrode materials. Literature [26] used composite nanomaterials formed by carbon nanotubes and platinum to act as the cathodic catalyst for MFC, and the cathodic catalytic effect of MFC was optimal under the concentration condition of 0.3 mg/cm², with high COD removal rate (88%), which provides a pathway for the production of sustainable clean energy.

In the carbon nanofiber-based MFC performance enhancement, literature [27] found that 600°C heat treatment of nitrogen-doped electrostatically spun carbon nanofibers reduced the treatment cost in addition to maintaining the original excellent performance, while the treated carbon nanofibers enhanced the anode electrode bacterial growth performance of single-compartment MFC. Literature [28] used multi-walled carbon nanotube-carbon nanofiber composite nanomaterials as MFC anode materials to obtain the maximum power density (362.20 mW/m²), which enhanced the microbial attachment strength and electron transfer capability. Literature [29] combined cobalt-nickel alloy, nitrogen-doped carbon nanotubes, and carbon nanofibers to fabricate three-dimensional layered graphitic carbon, which achieved the maximum power density (210045 mW/m²) and can be used as an MFC air cathode catalyst to enhance MFC performance. In addition, literature [30] prepared iron/iron oxide nanoparticles with nitrogen-doped carbon quantum dots as an anode material for MFC, which showed high performance in microbial attachment, electron transfer, and could convert waste microorganisms into green energy, and achieved the maximum power density (836 mW/m²). Literature [31] embedded low-cost and sustainable plant carbon dots, a carbon-based nanomaterial, into the MFC anode catalysis and improved the output power and wastewater treatment of MFC.

In this paper, microbial fuel cells are optimized using nanocarbon materials. Based on the preparation of multiple types of experimental materials, the microbial fuel cell is constructed and activated for complex wastewater treatment experiments. The performance advantages of the constructed cell are verified from two dimensions, electrochemical analysis and water quality analysis. Analyze the power production performance of anode materials such as L-N/PCs in combination with cyclic voltammetry test. Compare the magnitude of internal resistance of anode materials etc. by polarization and power density test. The water purification ability of multiple microbial fuel cells is measured by COD, TN, and TP removal rates to determine the advantages of L-N/PCs-MFC for wastewater treatment.

II. Pre-laboratory preparation

This chapter lays the foundation for subsequent modeling and analysis of wastewater treatment through preexperimental material preparation and microbial fuel cell construction.

II. A.Materials purchased for the experiment

II. A. 1) Experimental materials

Polyacrylonitrile graphite felts with pore size 205-305 μm, thickness 5 mm, carbon content 99%, purchased from Beijing Sanye Carbon.

Multi-walled carbon nanotubes (MWCNT) OD <8.5 nm, purity >96%, purchased from Chengdu Organic Chemistry Co.

Graphite rods 7mm in diameter, 10cm in length, 99.9% carbon content, purchased from Curious Teaching Laboratory Equipment.

DuPont Nafion117 proton exchange membrane with thickness of 185 μm, density of 365 g/m², conductivity of 0.085 s/cm, exchange capacity of 0.90 meq/g, purchased from Beijing Fengxiang Technology Co.

Sodium acetate anhydrous, yeast extract, sodium bicarbonate, potassium dihydrogen phosphate were purchased from Tianjin Hengxing Chemical Reagent Manufacturing Co., Ltd; potassium chloride, magnesium chloride were purchased from Tianjin Kemi Chemical Reagent Co., Ltd; disodium phosphate dodecahydrate, disodium phosphate dihydrogen dihydrate, potassium ferricyanide, potassium ferrocyanide and aniline were purchased from China National Pharmaceutical Corporation Chemical Reagent Co.

High-purity nitrogen (99.99%) was purchased from Henan Keyi Gas Engineering Co.

II. A. 2) Experimental reagents

Microbial fuel cell (MFC) anode liquid: sodium acetate 1.65g/L, yeast extract 3.0g/L, potassium dihydrogen phosphate 0.5g/L, sodium bicarbonate 2.6g/L, potassium gasification 0.2g/L, magnesium gasification 0.2g/L, calcium gasification 0.2g/L. Prepare 260mL of anode liquid, plug the mouth of the bottle with cotton, and then wrapped in newspaper and cotton thread intact, sterilized at 120℃. Sterilize at 120℃ for 25min, and store in refrigerator at 5℃ for spare.

MFC cathode solution: 0.06M potassium ferricyanide, 0.15M potassium chloride, dissolved and fixed in 260mL brown wide-mouth bottles, stored at room temperature.

PBS reserve solution (60mMPBS): weigh 0.2965g of sodium dihydrogen phosphate dihydrate, 2.899g of disodium hydrogen phosphate dodecahydrate, first dissolve with ultrapure water, then adjust PH to 7.4, and finally volume to 260mL, put it in a triangular flask and seal it with aseptic film, sterilize it at 120C for 25min, and put it into the refrigerator at 5℃ for storage.

PBS solution (20mMPBS): Dilute the PBS solution 3 times with ultrapure water.

Potassium ferricyanide solution: 6mM potassium ferricyanide, 2M potassium chloride, dissolve and set in a brown bottle, store at room temperature. All the above solutions are prepared with ultrapure water.

II. B.Preparation of the anode material

II. B. 1) Preparation of nitrogen-doped porous carbon materials

1) Drugs used in the experiment

The reagents used in the experiment included melamine, sodium citrate dihydrate and L-cysteine, all of which were chemically pure. Melamine and sodium citrate dihydrate were produced by Sinopharm Chemical Reagent Co. and L-cysteine was produced by Shanghai McLean Biochemical Technology Co.

2) Material preparation steps

(1) Preparation of N/PCs

Weigh sodium citrate solid and melamine solid (mass ratio 15:1), mix them and put them into a mortar and grind them to make a homogeneous mixture. The mixture was put into a magnetic cup, calcined in a tube furnace under argon atmosphere at an elevated temperature (6 ℃/min) to 850 ℃ for 6 hours, after cooling down, the product was ground and washed with dilute hydrochloric acid, then rinsed with deionized water, pumped and filtered, and then dried at 85 ℃ in a vacuum drying oven for 10 hours, nitrogen-doped porous carbon materials (N/PCs) were prepared.

(2) Preparation of L-N/PCs

Sodium citrate solid and L-cysteine solid (mass ratio 15:1) were weighed and mixed into a mortar and pestle to make a homogeneous mixture. The mixture was put into a magnetic cup and calcined in a tube furnace under argon atmosphere at an elevated temperature (6 °C/min) to 850 °C for 6 h. After cooling down, the product was ground and washed with dilute hydrochloric acid, then rinsed with deionized water, filtered and dried in a vacuum drying oven at 85 °C for 10 h. Nitrogen-doped porous carbon materials (L-N/PCs) were prepared.

(3) Preparation of porous carbon materials (PCs) for comparison materials

Several sodium citrate solids were weighed and ground in a mortar. Put the sodium citrate powder into the magnetic cup, in the tube furnace, argon atmosphere, heating (6 ℃ / min) to 850 ℃ calcination for 6 hours, after cooling down, the product will be ground with dilute hydrochloric acid cleaning, and then rinsed with deionized water, filtration in a vacuum drying oven at 85 ℃ after drying for 10 hours to prepare the contrasting material porous carbon materials (PCs).

3) Preparation of composite materials used as electrodes for modified anodes

Take two centrifugal tubes, each centrifugal tube were measured 20uL Nafion solution and 120uL ultrapure water, and then weighed 15mg N/PCs, L-N/PCs and PCs materials (used for modification of the carbon cloth anode), were placed into the three centrifugal tubes, manually mixed and then placed into the ultrasonic instrument in the ultrasonic 45min, to form N/PCs slurry, L-N/PCs slurry and PCs slurry, the three parts of the slurry, and the three parts of the slurry, the three parts of the composite material as a modification of the electrode. PCs slurry, the three

slurries were applied to the three treated carbon cloths (all slurries were applied to the carbon cloths as much as possible), and air-dried or low-temperature dried for spare.

II. B. 2) Preparation of biomass carbon materials

1) Drugs used in the experiment

The reagents used in the experiment included rice bran (produced in Nanchang farmland, Jiangxi Province), potassium hydroxide (chemically pure, Xilong Chemical Co., Ltd.).

2) Steps of material preparation

First, the rice bran was pretreated by submerging it in 5 M potassium hydroxide solution for 60 min, then rinsed with deionized water, filtered and vacuum dried. Weighing the same mass of pretreated rice bran 3 parts, in the tube furnace, argon atmosphere, respectively, temperature (6 ℃ / min) to 750 ℃, 850 ℃, 950 ℃, 1050 ℃ calcined for 2.5 hours, to produce carbon materials containing aluminum, calcium, silicon, and oxygen and other mixed elements.

3) Preparation of composite materials used as modified anode electrodes

Take two centrifugal tubes, each centrifugal tube were measured 20uL Nafion solution and 120uL ultrapure water, and then weighed 15mg M/PC750-PCs, M/PC850-PCs, M/PC950-PCs, and M/PC1050-PCs materials (used for modification of the anode of the carbon cloth), were placed into four centrifugal tubes, and then manually mixed before being put into the Ultrasonic instrument in the ultrasonic 45min, the formation of M/PC750-PCs slurry, M/PC850-PCs slurry, M/PC950-PCs slurry and M/PC1050-PCs slurry, four copies of the slurry were coated to the four treated carbon cloth (as far as possible all the slurry coated to the carbon cloth), air-drying or low-temperature drying standby.

II. C. Construction and startup of microbial fuel cells

II. C. 1) Construction of microbial fuel cells

The dual chamber microbial fuel cell consisted of two reaction tanks of the same volume (65mL). A proton exchange membrane 2.5 cm × 5 cm (12.5 cm²) formed a sandwich structure with the two reaction tanks. Bare graphite felts or graphite felts modified with carbon nanotubes and polyaniline were used as the anode of the microbial fuel cell, and carbon fiber cloth 2.5 cm × 5 cm (12.5 cm²) was used as the cathode of the microbial fuel cell to construct different microbial fuel cells. The anode chamber was enriched with anode solution inoculated with Schizosaccharomyces pombe. The cathode chamber had 50 mL of cathode solution (0.05 M K3[Fe(CN)6]/0.1 MKCl). The microbial fuel cell was placed in a constant temperature incubator at 35°C, and the anode solution was continuously magnetically stirred at a stirring rate of 550 r/min.

II. C. 2) Start-up of microbial fuel cells

A constant resistance of 1.95 kΩ is applied between the cathode and anode to make the connection, data is collected through USB data collector and voltage data is displayed through computer related software and real time voltage data is monitored.

III. L-N/PCs-MFC's wastewater treatment capacity practice

In this chapter, the constructed microbial fuel cell is put into practice for wastewater treatment, and the enhancement of microbial fuel cell by nanocarbon materials is analyzed in terms of both electrochemical performance and water purification effect.

III. A. L-N/PCs running on MFCs

III. A. 1) L-N/PCs-MFC construction

The coated anode materials L-N/PCs, PCs and blank carbon cloth with uncoated materials were used as anodes, and the three anodes were placed in the same anode chamber, and carbon brushes were used as cathodes, which were fixed with titanium wires to the anode and cathode chambers, respectively, with a resistance value of 650 Ω of the external resistance, and the microorganisms were stabilized to grow on the surface of the anode materials over time, and decreased the resistance value in order, with 550 Ω, 450 Ω, 350 Ω, 350 Ω, and 250Ω, 150Ω, 15Ω, 5Ω, to the anode microorganisms generate a microbial film resistant to high current passage.

III. A. 2) Results of performance testing of L-N/PCs in MFCs

Figure 1 shows the XRD pattern and Raman pattern of L-N/PCs. Figure 1(a) demonstrates the X-ray diffraction (XRD) pattern of L-N/PCs, where two broad diffraction peaks are observed in 16.4° and 40.8°, corresponding to the reflective crystal planes of (001) and (101) carbon, respectively. The absence of other impurity peaks indicates that the impurity ions have been removed. Fig. 1(b) is the Raman profile of L-N/PCs and PCs showing two peaks located

between 1245.6 cm^{-1} and 1518.2 cm^{-1} from defective carbon (sp^3) and graphitic carbon (sp^2) atoms, respectively. The density ratio of the two peaks (ID/IG) is usually used to evaluate the defect density of carbon. The ID/IG of L-N/PCs is higher than that of PCs, which implies that the nitrogen dopant in L-N/PCs produces more defective structures in L-N/PCs. Combining the specific surface areas of L-N/PCs and PCs, it was found that the specific surface area of L-N/PCs was larger, suggesting that the defects in L-N/PCs could provide a high density of active sites.

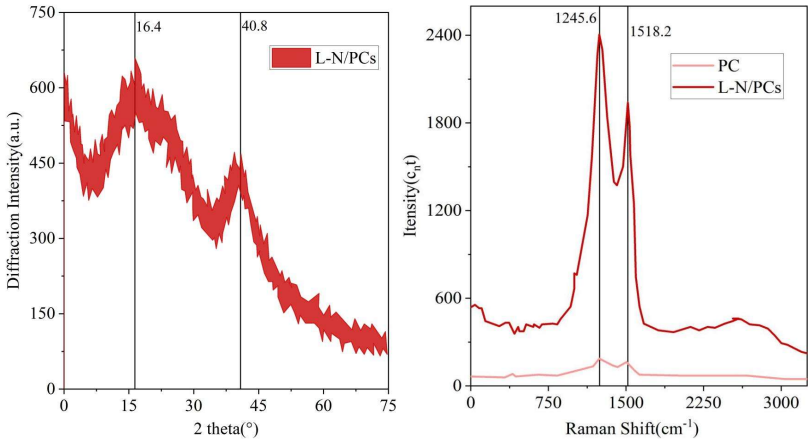

(a) XRD pattern of N/PCs of MFCs (b) Raman spectra of N/PCs of MFCs

Figure 1: XRD pattern and Raman spectra of N/PCs of MFCs

III. B. Indicators and methods of analysis

III. B. 1) Electrochemical analysis methods

1) Output Voltage

A paperless recorder is used to determine the voltage of the MFC wastewater treatment system, the output voltage of the system is collected every minute and the collected data is stored in the paperless recorder.

2) Output current

The current is calculated by Ohm's law with the following formula:

$$I = \frac{U}{R} \tag{1}$$

where: I - output current, A , U -Output voltage, V , R -external resistance, Ω .

3) Tafel (Tafel) curve

The Tafel curve represents the relationship between current and potential for different electrodes, and its physical meaning is the degree of electrode potential that needs to be changed to achieve a certain current. In this thesis, the Tafel curve of the anode was determined using an electrochemical workstation. The working electrode is an anodic carbon brush, the counter electrode is a cathodic carbon brush, and the reference electrode is an Ag/AgCl electrode, which is placed between the working electrode and the counter electrode. The potential scanning speed was 1.2mV/s, and the membrane potential scanning range was 0~100mV. Then the Tafel curve was plotted with the voltage as the horizontal coordinate and the logarithm of the reciprocal of the current as the vertical coordinate.

4) Polarization curve

Polarization curve can be used to characterize the relationship between the output voltage of the coupled wastewater treatment system and the current density, reflecting the output voltage of the coupled wastewater treatment system with the increase in current changes, is an important characterization of the electrical performance of the MFC wastewater treatment system. In this paper, the output voltage of the MFC sewage treatment system is recorded after each change of resistance by changing the resistance, and then the polarization curve is drawn with the current as the horizontal coordinate and the voltage as the vertical coordinate.

5) Power density

Volumetric power density is used in this experiment and is calculated as follows:

$$P = \frac{U^2}{RV} \tag{2}$$

Where, P -volume power density, W/m^3, U -Total voltage at the output, V, R -Total external resistance, Ω, V - effective volume, m^3.

The power density curve is then plotted with current as the horizontal coordinate and power density as the vertical coordinate.

III. B. 2) Methods of water quality analysis

1) Determination of chemical oxygen demand (COD)

In this experiment, COD was measured by multiparameter water quality meter, 2.0mL of water samples to be tested and blank distilled water samples were taken and added into different colorimetric tubes, the solution was fully mixed by shaking and shaking after adding the elimination reagents into the colorimetric tubes, and then put into the elimination instrument for elimination for 15min; after the elimination was completed, the colorimetric tubes were taken out for cooling and 2.0mL of distilled water was added; after the cooling was completed, the COD was determined by using blank distilled water samples. After cooling, use the blank distilled water sample to calibrate the multi-parameter water quality meter, and then put in the water sample to be measured for COD determination.

2) Ammonia nitrogen determination

In this experiment, ammonia nitrogen was measured by multiparameter water quality tester, 15mL of water samples to be tested were taken from blank distilled water samples to be added into different colorimetric tubes, 1.5mL of ammonia nitrogen special detection reagent was added into each of the colorimetric tubes, and the test reagents were shaken well and left to stand for 15 minutes, and then the practical blank distilled water samples were used to calibrate the multiparameter water quality tester, and then put into the water samples to be tested to be measured for ammonia nitrogen determination.

3) Determination of total nitrogen (TN) and total phosphorus (TP) water quality indicators

In this experiment, TN and TP were measured by automatic chemical analyzer.

III. C. L-N/PCs-MFC electrochemical performance testing

III. C. 1) Cyclic Voltammetry

Based on the different shapes, peak potentials, peak currents and peak areas presented by the CV curves, information about the specific capacitance of the electrodes, the activity of the electroproducing microorganisms, the reaction mechanism on the electrode surface, and whether or not the reaction is reversible can be analyzed. Figure 2 shows the test results. From the figure, it can be seen that the CV curves of the two groups of anode-modified MFCs showed relatively obvious redox peaks at -0.45 V and 0.5 V voltage. Among them, the peak area of L-N/PCs anode MFC was the largest, and N/PCs anode MFC was the second largest.

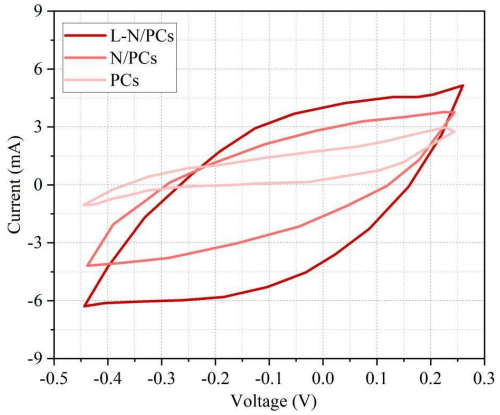

Figure 2: Cyclic voltammetry curves of three sets of electrodes as MFC anodes

The unmodified PCs, on the other hand, showed no obvious redox peaks, which indicates that the L-N/PCs anode MFC possesses the largest specific capacitance, which is closely related to the high capacitance property of L-N/PCs itself. In addition, at the same voltage (e.g., 0.1 V and -0.1 V), the response current values of the L-N/PCs anode MFCs are also consistently the highest (4.5 mA and 3.05 mA), followed by the N/PCs, and the smallest for the PCs. It is well known that current is generated by electron migration, therefore, a higher current value means that more electron migration was generated, which indicates that the electricity-producing microorganisms on the surface of the L-N/PCs anode have a stronger electron output capacity, and at the same time, a higher peak current represents a stronger biofilm activity, so this also indicates that the amount of active microorganisms on the L-N/PCs

anode material is the highest, and the electrons are constantly generated and transferred to the anode. This is attributed to the unique structure of L-N/PCs anode which provides a better survival and metabolism place for the microorganisms, and on the other hand, the excellent hydrophilicity and biocompatibility of L-N/PCs anode accelerates the diffusion of molecules in the anode liquid on the electrode, and the two factors synergize with each other to jointly improve the performance of MFCs in terms of electricity production.

III. C. 2) Polarization and power density tests

In order to further investigate the influence of L-N/PCs and N/PCs modified anodes on the overall performance of MFC, the polarization and power density curves of N/PCs, L-N/PCs, PCs three groups of electrodes and MFC were measured by steady state method after the stable operation of the battery, in the polarization area diagram, if there is a sudden drop in the voltage, it indicates that the anode is polarized. The output power density of MFC was calculated based on the area of anode and PCs. area of the electrode was calculated.

Figure 3 shows the polarization curves of MFCs at the three sets of electrodes. The highest points of the three curves indicate the open-circuit voltage (OCV) of the three groups of MFCs, and the open-circuit voltages of the L-N/PCs, N/PCs, and PCs anode MFCs are 820.59 mV, 767.14 mV, and 751.10 mV, respectively. Comparing the three polarization regions in the figure, it can be seen that the slope of the polarization curve of the L-N/PCs anode MFC is smaller than that of the other two groups, and the degree of polarization is larger than that of the other two groups of electrodes. Moreover, from the open-circuit voltage, the open-circuit voltage of the L-N/PCs anode MFC is 53.45 mV and 69.49 mV higher than that of the N/PCs anode and the PCs anode MFC, respectively, indicating that the L-N/PCs anode MFC has the smallest internal resistance during the whole operation.

It is shown that the internal resistance of MFC is mainly composed of three parts, activation internal resistance, ohmic internal resistance and diffusion internal resistance, and similarly the polarization curve is divided into three parts, namely, activation polarization region, ohmic polarization region and diffusion polarization region. The activation internal resistance is mainly related to the activation reaction rate on the electrode surface; the ohmic internal resistance is mainly related to the electrode material, the cathode and anode chamber solutions and the proton exchange membrane; and the diffusion internal resistance, also known as the concentration internal resistance, is mainly related to the ion diffusion rate or charge transport efficiency. As can be seen in Fig. 3, the slopes of the polarization curves of the three groups of MFCs changed less throughout the reaction process, which was analyzed to be due to the fact that in the activation polarization region, the activation reaction rate on the electrode surface was larger, especially more active sites on the anode surface of the L-N/PCs accelerated the reaction rate on the surface of the electrodes, which resulted in a lower activation internal resistance. In the ohmic polarization zone, the ohmic internal resistance mainly comes from the transfer resistance of electrons and protons, and the three groups of MFCs have the same conditions except for the different anode materials, and the difference in anode materials determines the difference in the electron generation and transfer ability, and the size of the electron generation and transfer ability of the three groups of electrodes is in the order of L-N/PCs>N/PCs>PCs>PCs, so that the size of the ohmic internal resistance of the three groups of electrodes is L-N/PCs<N/PCs<PCs. In the diffusion polarization zone, the diffusion internal resistance mainly comes from the mass transfer resistance of reactants and products, thanks to the good hydrophilicity and biocompatibility of the L-N/PCs electrode, which accelerates the infiltration of the anode liquid on the electrode and the diffusion of ions, strengthens the adhesion of the electroproducing microorganisms on the surface of the anode, and improves the electron transfer ability to the anode, which greatly reduces the diffusion internal resistance, and therefore no modification of the polarization curves is found in the results of the tests. Therefore, no polarization phenomenon was found in the polarization curves of the modified electrode.

Since the factors affecting the activation internal resistance and diffusion internal resistance during the whole MFC operation process are relatively small, the ohmic internal resistance caused by the different anode materials becomes the main influencing factor, which makes the slope of the whole polarization curve change in a single way.

Fig. 4 shows the power density curves of MFC with three sets of electrodes. From Fig. 4, it can be seen that at a current density of 928.15 mA•m² , the PCs electrode MFC obtained the maximum power density of 706.31 mW•m² ; at a current density of 2085.37 mA•m² , the N/PCs electrode MFC obtained the maximum power density of 1674.14 mW•m²; at a current density of 1992.70 mA•m², the L-N/PCs electrode MFC obtained a maximum power density of 2022.20 mW•m². Compared to the PCs electrode MFC, the L-N/PCs electrode MFC and the N/PCs electrode MFC obtained a maximum power density of 2022.20 mW•m². PCs electrode MFC increased the maximum power density by 186.30% and 137.03%, respectively. Obviously, the L-N/PCs electrode MFC possesses the highest output power density. Since the power density of MFC is proportional to the square of the voltage and inversely proportional to the internal resistance of the system and the anode area, this indicates that the composite of L-N/PCs reduces the internal resistance of the system and improves the anode mass-transfer efficiency, and it also indicates that per unit area of the anode material, the N/PCs electrode hosts more power-producing microorganisms than the other two

groups of electrodes, provides more active sites, the reaction rate of the electrode surface is faster, the power-producing microorganisms have a stronger ability to reproduce and metabolize, and the MFC output power density is higher, which is consistent with the results of the CV and polarization tests.

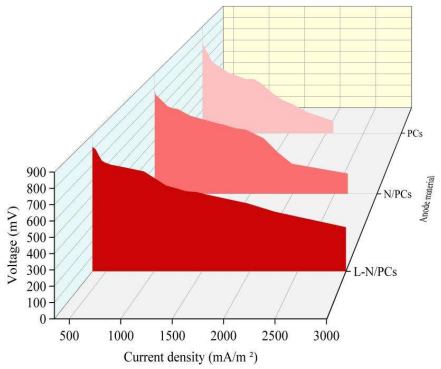

Figure 3: Polarisation curves of MFC at three sets of electrodes

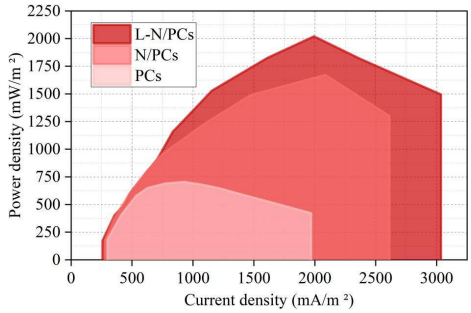

Figure 4: Power density profile of MFC with three sets of electrodes

III. D. L-N/PCs-MFC water purification effect test

III. D. 1) COD removal

Figure 5 shows the COD removal rate in MFC with different substrate concentrations. From Fig. 5, it can be seen that the COD removal rate of L-N/PCs reactor was higher than that of control N/PCs reactor and PCs reactor, indicating that the L-N/PCs electrode is more favorable for COD degradation in MFC, and it is the addition of L-N in MFC that promotes the removal of COD in the reactor.

The total COD was 5657.24 mg/L in the C1 case, 7259.05 mg/L in the C2 case, and 9132.35 mg/L in the C3 case. Among the L-N/PCs, N/PCs, and PCs reactors in the three different substrate cases with different carbon amounts (C1, C2, and C3), C2-L-N/PCs had the COD removal was the highest at 44.12%, N/PCs reactor COD removal was 23.22%, and PCs reactor was 39.08%.C1 had the second highest COD removal, L-N/PCs and PCs had COD removal of 35.04% and 31.28%, respectively; and N/PCs had 16.18%.C3 had the lowest COD removal, L-N/ PCs, PCs with COD removal of 20.70%, 21.72%, and N/PCs with 10.34%, which may be due to the high concentration, resulting in the inactive growth of the bacterial colony, which makes the COD degradation efficiency lower than the rest of the concentration.

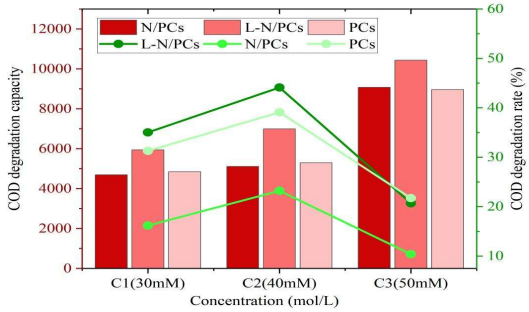

Figure 5: COD removal rate of MFC with different substrate concentrations

III. D. 2) TN and TP removal rates

Figure 6 shows the TP removal in the L-N/PCs-MFC system during the 65-day experimental cycle. The TP removal in L-N/PCs-MFC was greatly affected at the beginning of the experiment. The graph shows that the TP removal rate was high and low during the first 19 days of the experiment, with a maximum of about 0.92 and a minimum of 0.25. This is due to the instability of the microbial community associated with TP removal under the stress of antibiotics. From about day 19 to day 43, the TP removal efficiency of L-N/PCs-MFC began to gradually increase from about 0.82 to a maximum of about 0.99 as the antibiotic tolerance of bacteria increased. After the 43rd day, the TP removal efficiency of L-N/PCs-MFC decreased, but still maintained above 0.75. From the TP removal experiments, it can be seen that L-N/PCs-MFC has a good effluent purification effect and high microbial activity, which can persist for at least 65 days or more.

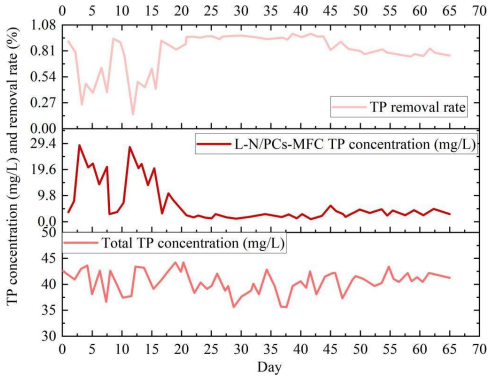

Figure 6: The removal situation of TP in the L-N/PCs-MFC system

Figure 7 shows the TN removal in the L-N/PCs-MFC system. During the first 23 days or so at the beginning of the experiment, the TN removal in the L-N/PCs-MFC fluctuated considerably, reaching a high of 0.91 and a low of only 0.41. TN removal from L-N/PCs-MFC was consistently above 0.8 during the 23-65 day end-of-experiment period, with removal closer to 0.9 for most of the time. This indicates that the TN removal effect of the L-N/PCs-MFC system is superior, and at the same time, the microbial activity in it was again verified.

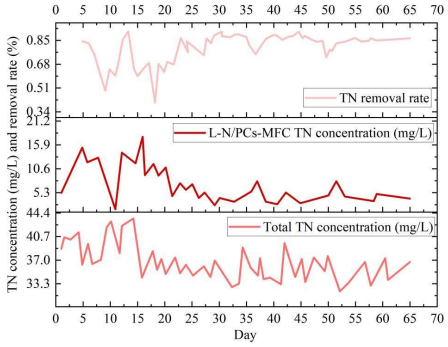

Figure 7: The removal situation of TN in the L-N/PCs-MFC system

IV. Conclusion

In this paper, carbon nanomaterials were added to microbial fuel cells (MFCs) to realize the efficient purification of complex wastewater. Through several sets of tests, it was found that the CV curves of L-N/PCs-MFC showed obvious redox peaks at both -0.45 V and 0.5 V voltage, and the peak area and specific capacitance were the largest. The open-circuit voltages of L-N/PCs-MFC showed an increase of 53.45 mV and 69.49 mV compared with the other 2 types of cells, and the operation internal resistance was the smallest. The COD removal rates at 3 different The removal rates of TN and TP fluctuated greatly in the early stage of the experiment, but were maintained at a high level in the middle and late stages of the experiment. The L-N/PCs-MFC constructed in this paper was able to realize the full purification of complex wastewater. The purification rate of this cell can be further improved in the future to realize the rapid purification of complex sewage.

References

[1] Li, J., See, K. F., & Chi, J. (2019). Water resources and water pollution emissions in China's industrial sector: A green-biased technological progress analysis. Journal of cleaner production, 229, 1412-1426.

[2] Okorogbona, A. O., Denner, F. D., Managa, L. R., Khosa, T. B., Maduwa, K., Adebola, P. O., ... & Macevele, S. (2018). Water quality impacts on agricultural productivity and environment. Sustainable Agriculture Reviews 27, 1-35.

[3] Lin, L., Yang, H., & Xu, X. (2022). Effects of water pollution on human health and disease heterogeneity: a review. Frontiers in environmental science, 10, 880246.

[4] Mooij, W. M., van Wijk, D., Beusen, A. H., Brederveld, R. J., Chang, M., Cobben, M. M., ... & Teurlincx, S. (2019). Modeling water quality in the Anthropocene: directions for the next-generation aquatic ecosystem models. Current Opinion in Environmental Sustainability, 36, 85-95.

[5] Zawadzka, J., Gallagher, E., Smith, H., & Corstanje, R. (2019). Ecosystem services from combined natural and engineered water and wastewater treatment systems: Going beyond water quality enhancement. Ecological Engineering, 142, 100006.

[6] Wear, S. L., Acuña, V., McDonald, R., & Font, C. (2021). Sewage pollution, declining ecosystem health, and cross-sector collaboration. Biological Conservation, 255, 109010.

[7] Hurynovich, A., Kwietniewski, M., & Romanovski, V. (2021). Evaluation of the possibility of utilization of sewage sludge from a wastewater treatment plant–case study. Desalination and Water Treatment, 227, 16-25.

[8] Hamawand, I. (2023). Energy consumption in water/wastewater treatment industry—optimisation potentials. Energies, 16(5), 2433.

[9] Poblete, I. B. S., Araujo, O. D. Q. F., & de Medeiros, J. L. (2022). Sewage-Water treatment and Sewage-Sludge management with power production as bioenergy with carbon capture system: A review. Processes, 10(4), 788.

[10] Rout, P. R., Zhang, T. C., Bhunia, P., & Surampalli, R. Y. (2021). Treatment technologies for emerging contaminants in wastewater treatment plants: A review. Science of the Total Environment, 753, 141990.

[11] Li, W., Li, L., & Qiu, G. (2017). Energy consumption and economic cost of typical wastewater treatment systems in Shenzhen, China. Journal of Cleaner Production, 163, S374-S378.

[12] Zhang, X., Zhang, M., Liu, H., Gu, J., & Liu, Y. (2019). Environmental sustainability: a pressing challenge to biological sewage treatment processes. Current Opinion in Environmental Science & Health, 12, 1-5.

[13] He, L., Du, P., Chen, Y., Lu, H., Cheng, X., Chang, B., & Wang, Z. (2017). Advances in microbial fuel cells for wastewater treatment. Renewable and Sustainable Energy Reviews, 71, 388-403.

[14] Hamedani, E. A., Abasalt, A., & Talebi, S. (2024). Application of microbial fuel cells in wastewater treatment and green energy production: a comprehensive review of technology fundamentals and challenges. Fuel, 370, 131855.

[15] Wang, Y., Zhang, H., Li, B., & Feng, Y. (2018). Integrating sludge microbial fuel cell with inclined plate settling and membrane filtration for electricity generation, efficient sludge reduction and high wastewater quality. Chemical Engineering Journal, 331, 152-160.

[16] Do, M. H., Ngo, H. H., Guo, W. S., Liu, Y., Chang, S. W., Nguyen, D. D., ... & Ni, B. J. (2018). Challenges in the application of microbial fuel cells to wastewater treatment and energy production: a mini review. Science of the Total Environment, 639, 910-920.

[17] Ewing, T., Ha, P. T., & Beyenal, H. (2017). Evaluation of long-term performance of sediment microbial fuel cells and the role of natural resources. Applied Energy, 192, 490-497.

[18] Goswami, R., & Mishra, V. K. (2018). A review of design, operational conditions and applications of microbial fuel cells. Biofuels, 9(2), 203-220.

[19] Zhang, Y., Liu, L., Van der Bruggen, B., & Yang, F. (2017). Nanocarbon based composite electrodes and their application in microbial fuel cells. Journal of Materials Chemistry A, 5(25), 12673-12698.

[20] Liao, H. X., Wei, H. X., Zhou, S. Q., Zhou, H. W., Cao, Y. T., & Li, N. (2025). Iron–Nitrogen Co-Doped Carbon Nanostructures for Applications in Oxygen Reduction Reactions and Microbial Fuel Cells. ACS Applied Nano Materials, 8(9), 4431-4440.

[21] Pareek, A., Sravan, J. S., & Mohan, S. V. (2019). Fabrication of three-dimensional graphene anode for augmenting performance in microbial fuel cells. Carbon Resources Conversion, 2(2), 134-140.

[22] Li, P., Li, X., Huang, J., Qu, W., Pan, X., Chen, Q., ... & Tao, H. (2022). Nitrogen-doped graphene oxide with enhanced bioelectricity generation from microbial fuel cells for marine sewage treatment. Journal of Cleaner Production, 376, 134071.

[23] Yaqoob, A. A., Ibrahim, M. N. M., Yaakop, A. S., Umar, K., & Ahmad, A. (2021). Modified graphene oxide anode: a bioinspired waste material for bioremediation of Pb2+ with energy generation through microbial fuel cells. Chemical Engineering Journal, 417, 128052.

[24] Fan, M., Zhang, W., Sun, J., Chen, L., Li, P., Chen, Y., ... & Shen, S. (2017). Different modified multi-walled carbon nanotube–based anodes to improve the performance of microbial fuel cells. international journal of hydrogen energy, 42(36), 22786-22795.

[25] Delord, B., Neri, W., Bertaux, K., Derre, A., Ly, I., Mano, N., & Poulin, P. (2017). Carbon nanotube fiber mats for microbial fuel cell electrodes. Bioresource technology, 243, 1227-1231.

[26] Ghasemi, M., Sedighi, M., & Tan, Y. H. (2021). Carbon nanotube/Pt cathode nanocomposite electrode in microbial fuel cells for wastewater treatment and bioenergy production. Sustainability, 13(14), 8057.

[27] Massaglia, G., Margaria, V., Fiorentin, M. R., Pasha, K., Sacco, A., Castellino, M., ... & Quaglio, M. (2020). Nonwoven mats of N-doped carbon nanofibers as high-performing anodes in microbial fuel cells. Materials Today Energy, 16, 100385.

[28] Cai, T., Huang, M., Huang, Y., & Zheng, W. (2019). Enhanced performance of microbial fuel cells by electrospinning carbon nanofibers hybrid carbon nanotubes composite anode. International journal of hydrogen energy, 44(5), 3088-3098.

[29] Li, J., Qian, J., Chen, X., Zeng, X., Li, L., Ouyang, B., ... & Zhang, W. (2022). Three-dimensional hierarchical graphitic carbon encapsulated CoNi alloy/N-doped CNTs/carbon nanofibers as an efficient multifunctional electrocatalyst for high-performance microbial fuel cells. Composites Part B: Engineering, 231, 109573.

[30] Habibi, M. F., Arvand, M., & Sohrabnezhad, S. (2021). Boosting bioelectricity generation in microbial fuel cells using metal@ metal oxides/nitrogen-doped carbon quantum dots. Energy, 223, 120103.

[31] Kumar, A., Narayanan, S. S., Thapa, B. S., Pandit, S., Pant, K., Mukhopadhyay, A. K., & Peera, S. G. (2022). Application of low-cost plant-derived carbon dots as a sustainable anode catalyst in microbial fuel cells for improved wastewater treatment and power output. Catalysts, 12(12), 1580.